International Journal of Engineering, Mathematical and Physical Sciences
ISSN: 2517-9934
Vol:12, No:2, 2018

Photoimpedance Spectroscopy Analysis of Planar and Nano-Textured Thin-Film Silicon Solar Cells

P. Kumar, D. Eisenhauer, M. M. K. Yousef, Q. Shi, A. S. G. Khalil, M. R. Saber, C. Becker, T. Pullerits, K. J. Karki

***Abstract*—**In impedance spectroscopy (IS) the response of a photo-active device is analysed as a function of ac bias. It is widely applied in a broad class of material systems and devices. It gives access to fundamental mechanisms of operation of solar cells. We have implemented a method of IS where we modulate the light instead of the bias. This scheme allows us to analyze not only carrier dynamics but also impedance of device locally. Here, using this scheme, we have measured the frequency-dependent photocurrent response of the thin-film planar and nano-textured Si solar cells using this method. Photocurrent response is measured in range of 50 Hz to 50 kHz. Bode and Nyquist plots are used to determine characteristic lifetime of both the cells. Interestingly, the carrier lifetime of both planar and nano-textured solar cells depend on back and front contact positions. This is due to either heterogeneity of device or contacts are not optimized. The estimated average lifetime is found to be shorter for the nano-textured cell, which could be due to the influence of the textured interface on the carrier relaxation dynamics.

***Keywords*—**Carrier lifetime, Impedance, nano-textured, and photocurrent.

I. Introduction

IS is well established tool for investigating the properties and qualities of many areas of materials science and devices, including inorganic, organic and biological systems [1], [2]. In IS, one analyses the current response of the device with respect to a modulated bias voltage, which provides an electrical impedance of materials systems and devices [3], [4]. In last two decades, IS has been extensively applied in dye-sensitized solar cells (DSCs) for studying the influence of electrode morphology, interfacial charge recombination and the charge transport [5]-[7]. Recently, Tripathi et al. [8] reported charge transfer and recombination kinetics in DSCs. Hamadani et al. [9] used intensity modulated photocurrent spectroscopy to investigate the dynamic of charge generation, recombination and transport in thin film CdTe/CdS solar cells. Due to its capability of separating the processes occurring at different parts of a solar cell, IS allows us to obtain important parameters affecting the cell performance, like the carrier conductivity, the lifetime, the diffusion coefficient, the diffusion length, the chemical capacitance and the recombination resistance.

In recent years, thin-film silicon solar cells on glass prepared by liquid-phase crystallization have made progress towards high efficiency solar cells [10]-[13]. But still the short-circuit current density as well as efficiency are less than the traditional Si solar cells. The reflection at the interface between glass superstrate and silicon absorber layer has been identified as one major loss mechanism [11], [14]. This optical loss can be reduced by nano-structuring of the interface between superstrate and absorber. Here, we have employed light modulated photocurrent spectroscopy (LMPS) to investigate charge carrier dynamics in planar and nano-texture interfaced thin film solar cells. LMPS is also known as photo-impedance spectroscopy where we modulate the excitation light instead of the bias and measure modulation frequency dependent photocurrent response. LMPS characterizes a solar cell by imposing a small perturbation on a steady-state illumination and measure the resultant photocurrent. The measurements are repeated across a range of perturbation frequencies to construct an LMPS spectrum.

The LMPS spectrum shows ability to cover a wide range of frequencies that allow us to distinguish various processes involved in transport recombination mechanisms of photoactive device. A specific model can be used to fit from low to high frequency regions, where each region represents different physical processes associated with distinct time constants. The high frequency response can be attributed to a high density of free carriers, particularly in a highly doped semiconductor, while the low-frequency response is commonly attributed to carrier captured/ released from deep traps and ionic transport [15]. Intermediate frequency response could be attributed for carrier captured or released by shallow defect states [16].

Analysis of LMPS spectrum is commonly presented in the form of the real (Re (Z)) and imaginary (Im (Z)) impedance corresponding to processes in and out of phase with the frequency modulated driving signal. It is established that solar cell shows complex impedance, therefore the knowledge of ac components of a solar cell under light illumination is not only important from fundamental point of view but also essential for developing an efficient system. In addition, the importance of dynamic response of charge carriers cannot be overestimated for the optimization of device. Thus, through knowledge of carrier dynamics (generation, diffusion, accumulation, recombination and transport) plays crucial role in the quality of the processed solar cells.

In LMPS, modulation of light instead of bias allows us to

Pushpendra Kumar, Qi Shi, Tonu Pullerits, and Khadga Jung Karki are with the Division of Chemical Physics and NanoLund, Lund University, Box 124, 22100, Lund, Sweden (e-mail: pushp07iitmandi@gmail.com).

David Eisenhauer and Christiane Becker are with the Helmholtz-Zentrum Berlin für Materialien und Energie, Albert-Einstein-Str. 16, 12489 Berlin, Germany.

Moataz M. K. Yousef and Ahmed S. G. Khalil are with the Center for Environmental and Smart Technology (CEST) and with the Physics Department, Faculty of Science, Fayoum University, Fayoum 63514, Egypt.

Mohamed R. Saber is with the Chemistry Department, Faculty of Science, Fayoum University, Fayoum 63514, Egypt.

determine carrier dynamics and impedance of device locally. The implementation of suitable solar cell model helps for LMPS data analysis as well as carrier dynamics. We have used two models, in which one nicely fits Nyquist and corresponding Bode plots of both planar and nano-textured and allow us to determine minority carrier lifetime. The method and results presented in this paper will be extended to image local impedance of the cells in the near future.

II. Experiments

Material: Nano-textured Si solar cells are produced by combining nano-imprint lithography of hexagonal nano-pillar arrays with spin-coating of titanium oxide layers. The details of fabrication of planar and nano-textured cells are given elsewhere [11].

Technique for data acquisition: The setup is based on the modulation technique described elsewhere [17]-[20]. Frequency dependent photocurrent response was measured using following set up as shown in Fig. 1. In brief, a continuous wave (CW) laser beam wavelength ~ 780 nm was used as the excitation light source obtained from Ti: sapphire oscillator (Synergy). The intensity of the Laser beam was modulated in the range of 50 Hz to 50 kHz by using an acousto-optic modulator. Excitation light was modulated in the form of square waves with help of a signal generator. After modulation, the beam was split into two parts using a 50:50 beam splitter. One part of the excitation beam was delivered to a silicon photodiode (PD1), which served as the reference signal while, another part was directed to the solar cells (PD2).

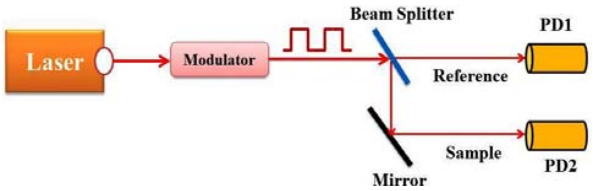

Fig. 1 Schematics of the setup used to measure the photocurrent response using light modulation

The photocurrent response from the sample was amplified by a pre-amplifier (SR570, Stanford Research Systems) and digitized at the rate of 2 MSa/s (mega samples per second). The photocurrent response at different modulation frequencies were obtained from the Fourier transform of the acquired data. The amplitude and the phase of the signal from the sample were measured with respect to the reference using the generalized lock-in amplifier [20]-[22]. Both the planar and the nano-textured devices were illuminated at zero bias conditions (0 V). All the measurements were performed at the room temperature with back side illumination.

III. Theory

In electrochemical IS technique, the excitation signal is perturbed with a small time-varying potential wave-form, which can be expressed as a function of time;

$$E_t = E_0 sin(\omega t) \quad (1)$$

where E_t is the potential difference at time t, E_0 is the amplitude of the voltage signal, and ω is the angular frequency given by ($\omega = 2\pi f$) expressed in radians/second and frequency, f, in hertz. The response signal has a phase shift (Φ) with amplitude of I_0 which can be expressed by;

$$I_t = I_0 sin(\omega t + \Phi) \quad (2)$$

Ohm's Law can be used to calculate the impedance (Z) of the system. The ratio of (2) to (1) is a complex number which determines the impedance at the corresponding frequency:

$$Z(\omega) = \frac{E_t}{I_t} = Z_0 \frac{sin(\omega t)}{sin(\omega t + \Phi)} \quad (3)$$

Thus, impedance can be expressed in terms of a magnitude Z_0 and a phase shift Φ. Using Euler's relations, equation (3) can be written as;

$$Z(\omega) = Z_0 exp(i\Phi) = Z_0(\cos\Phi + i\sin\Phi) \quad (4)$$

The impedance now is in the form of real part and imaginary part as follows,

$$Z_{Real} = \mathrm{Re}\,(Z) = Z_0 \cos(\Phi),$$
$$Z_{imaginary} = \mathrm{Im}\,(Z) = Z_0 \sin(\Phi) \quad (5)$$

From (5), the real and imaginary components of impedance and the phase angle depend on the range of frequency. For example, the resistive behavior lacks Im (Z) and its associated phase ($\Phi = 0^0$), while capacitive behavior lacks the Re (Z) and shows phase ($\Phi = -90^0$). For data analysis the real and imaginary part of impedance are expressed as Nyquist plot and Bode plot. Bode plot explicitly shows amplitude/phase of the signal in the frequency domain, while Nyquist plot represents a complex plane.

Model: In LMPS, the light intensity is modulated instead of the bias and corresponding photocurrent response is measured as a function of frequency. The response of the measured photocurrent can be represented as Nyquist and Bode plots for photoimpedance analysis. It is well established that the major processes governing carrier extraction in solid state crystalline solar cells are minority carrier diffusion and recombination. Therefore, in order to describe important processes of a solar cell, selection of the right model is one of the most essential steps. By considering those important processes, our photoimpedance data have been analyzed making use of the following models as shown in Fig. 2. The details of the models have been discussed n elsewhere [1], [23] and only a brief overview is given here. We have considered simple model A, which contains a recombination resistance (R_{rec}) and a chemical capacitance (C_μ), which directly indicates accumulation of minorities by the displacement of the Fermi level with respect to the respective band edge. The minority carrier lifetime (τ) can be determined using the relation, $\tau = R_{re.} C_\mu$ or $\omega = 1/\tau = R_{rec} C_\mu$, where ω is the angular frequency.

In this model, the frequency at the top of the arc in Nyquist plot corresponds to minority carrier lifetime. In the other model B, we considered a series resistance (R_s) that is usually associated with contacts and connected to R and C. R is a parallel resistance, which can be identified with the recombination resistance (R_{rec}), while C represents the parallel association of the chemical capacitance (C_μ) and the depletion-layer capacitance due to space–charge region. Actually, in IS, both the capacitances depend on the bias of the voltage. In the forward bias, chemical capacitance must dominate due to large concentration of minorities, while depletion-layer capacitance dominates at reverse bias.

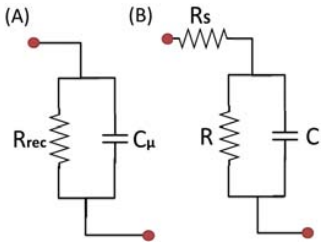

Fig. 2 The AC equivalent circuits for fitting experimental data of the planar and nanotexture solar cells

III. Results and Discussion

The modulation of the laser beam was produced by applying the square wave signals and corresponding photocurrent response was measured. The Fast Fourier transform (FFT) method was employed to detect signal and reference at certain range of frequency typically from 50 Hz to 50 kHz. FFT provides signal and reference at odd integer multiple of the frequencies set around 50 Hz (i.e. ~ 50 Hz, 150 Hz, 250 Hz, 350 Hz and so on) as shown in Fig. 3. Use of FFT allows fast local measurements of the impedance as opposed to the traditional method in which one applies perturbation only at a single frequency [24]. For all the LMPS measurements, we fixed the applied voltage bias across the device at 0 V i.e. short circuit condition and set the frequency scan range between 50 Hz and 500 KHz. During all the measurements laser power was kept at 10 µW. We have measured frequency dependent photocurrent response of both the cells at various positions of the back and front contacts using needle probe electrodes. Interestingly, all the measurements show position dependent photocurrent response. Therefore, we have measured photocurrent at five different positions of the contacts and averaged them to obtain the carrier lifetime. Experimental LMPS data were fitted using model A and B as presented in Fig. 2 to determine the carrier lifetime.

Fig. 3 shows LMPS spectrum of planar sample where Nyquist and corresponding Bode plots are fitted using model A (Bode plots are illustrated in the inset of Fig. 3). It is quite clear from Fig. 3 that model A is unable to fit entire range of frequencies; especially the mode does not fit the data at high frequencies.

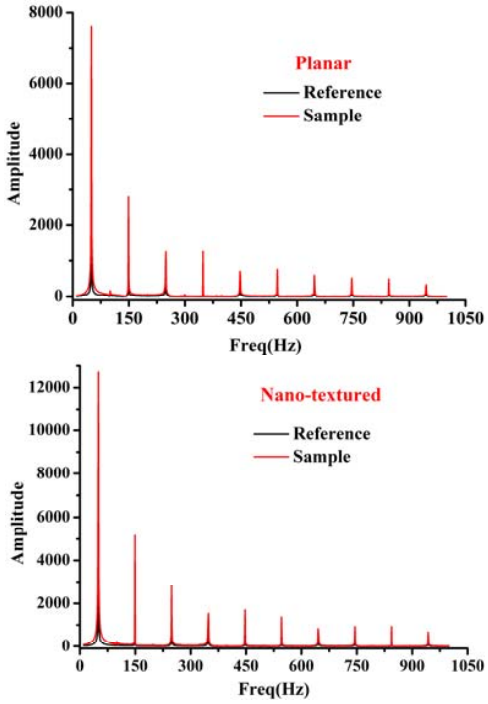

Fig. 2 Analysed FFT for photocurrent response of planar and nano-textured

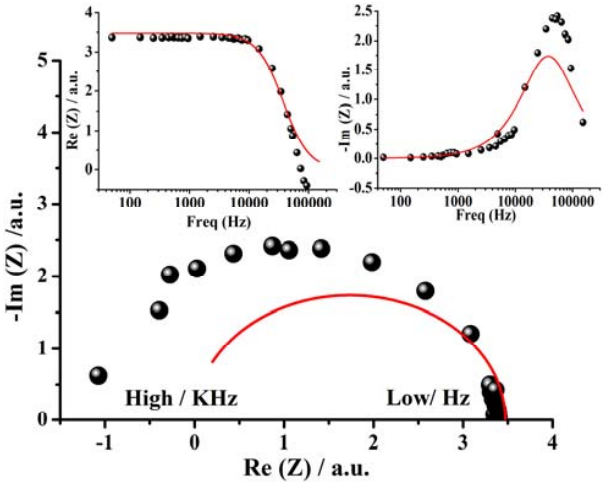

Fig. 3 Nyquist plot for planar and corresponding Bode plots are represented in the Inset of figure; the real part and the imaginary of the impedance. Measured data and the fitted data using model A represented by circles (black) and solid line (red), respectively

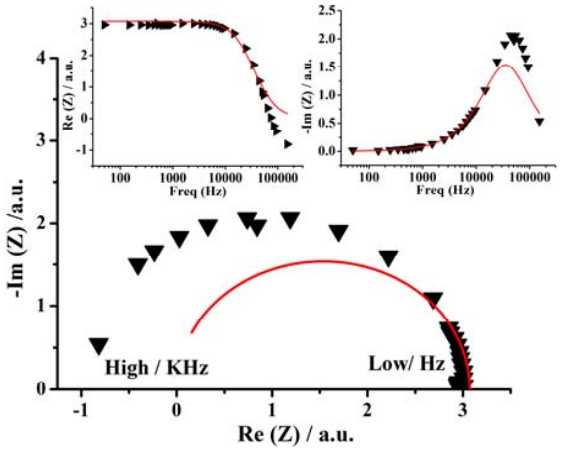

Fig. 4 Nyquist plot for nano-textured and corresponding Bode plots are represented in the Inset of figure; the real part and the imaginary part of the impedance. Measured data and the fitted data using model A represented by circles (black) and solid line (red), respectively

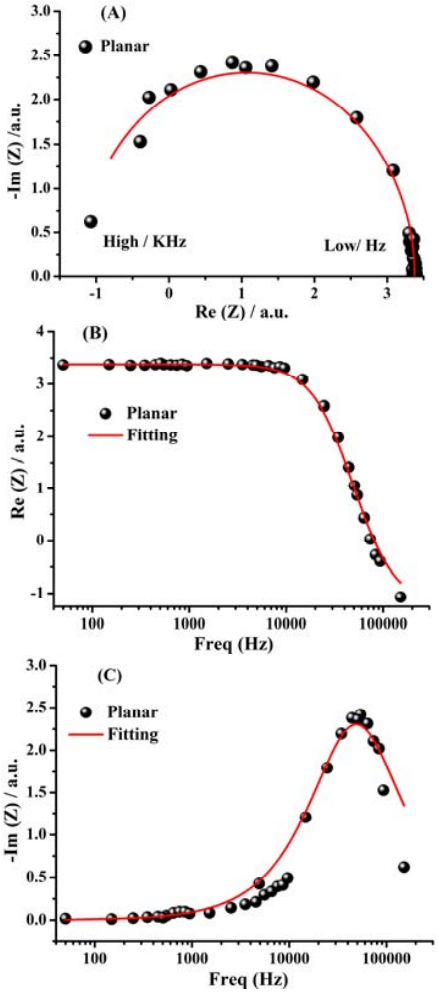

Fig. 5 Photoimpedance spectra of planar solar cell. a) Nyquist plot; the corresponding Bode plots for b) the real part and c) the imaginary of the impedance. Measured data and the fitted data using model B represented by circles (black) and solid line (red)

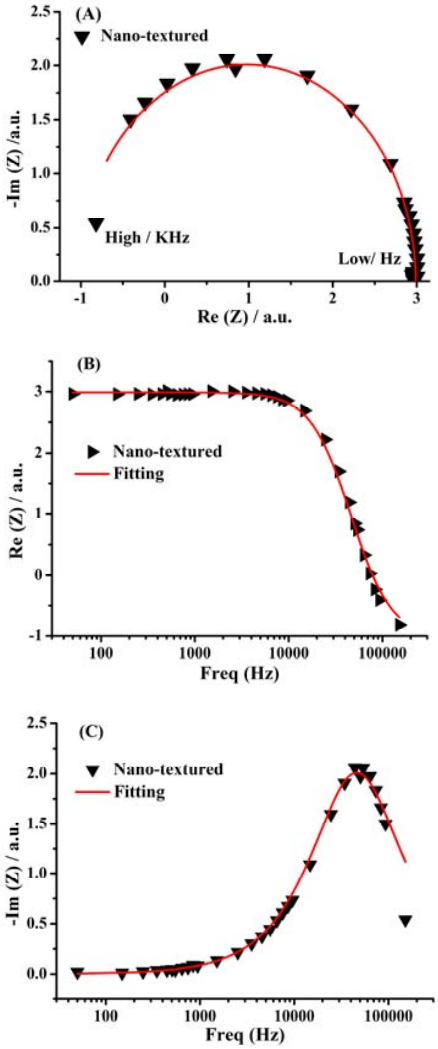

Fig. 6 Photoimpedance spectra of nano-textured solar cell. a) Nyquist plot; the corresponding Bode plots for b) the real part and c) the imaginary of the impedance. Measured data and the fitted data using model B represented by triangle (black) and solid line (red)

As shown in Fig. 4, this model also does not the fit the data from the nano-textured solar cell. Thus, it quite clear that model A is not appropriate to fit LMPS spectrum of neither the planar nor nano-textured cells. Therefore, in order to fit the entire range of frequencies, we need to modify it. According to the previous studies [23], [25], one can modify it by adding a series resistance (Rs) as illustrated in the Fig. 2. Consideration of the series resistance that is usually associated to contacts, improves the fitting of the curves at high frequencies as shown in Figs. 5 and 6. Fig. 5 shows the photoimpedance of the planar cell including Nyquist and corresponding Bode plots. The experimental data nicely fit with the predicted modal B. The estimated average carrier life time for planar cell is 26.7 ±4.7 µs.

The error is estimated from the standard deviation obtained from five independent measurements at the different front and back contact positions. Similar to the planar cell, we also have

employed the model to nano-textured solar cell as illustrated in the Fig.6. Nyquist and Bode curves fit well and the estimated average lifetime is found to be 21.5 ±3.5 μs. The existence of relatively high value of standard deviation for both planar and nanotexture clearly indicates that either contacts are not well optimized or film is not homogeneous. Nevertheless, the results indicate the carrier recombination in the planar cell is slightly slower compared to the nano-textured cell. The nanotexturing of absorber increases the surface area, which could be also increases the surface defects through which the carriers can recombine. In the previous report, Eisenhauer et al. [11] have found more absorption of light in nano-textured than planar reference.

IV. Conclusion

In summary, we employed LMPS to measure the frequency-dependent photocurrent response of the thin-film planar and nano-textured Si solar cells at several positions of back and front contacts. Bode and Nyquist plots were used to determine carrier lifetime by a using a specific solar cell model. Our results show that the carrier lifetime of both planar and nano-textured depends on contact positions, which clearly indicates that contacts are not optimized or films are not homogenous. This information is vital to control processing parameters and other related defects to optimize solar cell materials and processes, and thus performance. The estimated average lifetime is found to be longer in the planar solar cell compared to the nano-textured, which could be due to influence of the nano-textured interface on the carrier relaxation dynamics.

References

[1] I. Mora-Sero, G. Garcia-Belmonte, P. P. Boix, M. A. Vazquez and J. Bisquert, "Impedance spectroscopy characterisation of highly efficient silicon solar cells under different light illumination intensities," *Energy Environ. Sci.* 2(6), 678-686 (2009).

[2] J. Bisquert and V. S. Vikhrenko, "Interpretation of the Time Constants Measured by Kinetic Techniques in Nanostructured Semiconductor Electrodes and Dye-Sensitized Solar Cells," *J. Phys. Chem. B* 108(7), 2313-2322 (2004).

[3] J. Bisquert, G. Garcia-Belmonte, F. Fabregat-Santiago, N. S. Ferriols, P. Bogdanoff and E. C. Pereira, "Doubling Exponent Models for the Analysis of Porous Film Electrodes by Impedance. Relaxation of TiO2 Nanoporous in Aqueous Solution," *J. Phys. Chem. B* 104(10), 2287-2298 (2000).

[4] S. Soedergren, A. Hagfeldt, J. Olsson and S.-E. Lindquist, "Theoretical Models for the Action Spectrum and the Current-Voltage Characteristics of Microporous Semiconductor Films in Photoelectrochemical Cells," *J. Phys. Chem.* 98(21), 5552-5556 (1994).

[5] L. Dloczik, O. Ileperuma, I. Lauermann, L. M. Peter, E. A. Ponomarev, G. Redmond, N. J. Shaw and I. Uhlendorf, "Dynamic Response of Dye-Sensitized Nanocrystalline Solar Cells: Characterization by Intensity-Modulated Photocurrent Spectroscopy," *J. Phys. Chem. B* 101(49), 10281-10289 (1997).

[6] L. Bay and K. West, "An equivalent circuit approach to the modelling of the dynamics of dye sensitized solar cells," *Sol. Energy Mater. Sol. Cells* 87(1-4), 613-628 (2005).

[7] L. Peter, "Transport, trapping and interfacial transfer of electrons in dye-sensitized nanocrystalline solar cells," *J. Electroanal. Chem.* 599(2), 233-240 (2007).

[8] B. Tripathi, P. Yadav and M. Kumar, "Charge transfer and recombination kinetics in dye-sensitized solar cell using static and dynamic electrical characterization techniques," *Sol. Energy* 108(107-116 (2014).

[9] B. H. Hamadani, J. Roller, P. Kounavis, N. B. Zhitenev and D. J. Gundlach, "Modulated photocurrent spectroscopy of CdTe/CdS solar cells-equivalent circuit analysis," *Sol. Energy Mater. Sol. Cells* 116(126-134 (2013).

[10] Klaus Jäger, Grit Köppel, D. Eisenhauer, D. Chen, M. Hammerschmidt, S. Burger and C. Becker, "Optical simulations of advanced light management for liquid-phase crystallized silicon thin-film solar cells," in *SPIE Nanoscience + Engineering*, p. 7, Proc. SPIE (2017).

[11] D. Eisenhauer, K. Jaeger, G. Koeppel, B. Rech and C. Becker, "Optical Properties of Smooth Anti-Reflective Three-Dimensional Textures for Silicon Thin-film Solar Cells," *Energy Procedia* 102(27-35 (2016).

[12] G. Koeppel, D. Eisenhauer, B. Rech and C. Becker, "Tailoring Nano-Textures for Optimized Light In-Coupling in Liquid Phase Crystallized Silicon Thin-Film Solar Cells," *Phys. Status Solidi C* 14(10), n/a (2017).

[13] D. Eisenhauer, G. Köppel, K. Jäger, D. Chen, O. Shargaieva, P. Sonntag, D. Amkreutz, B. Rech and C. Becker, "Smooth anti-reflective three-dimensional textures for liquid phase crystallized silicon thin-film solar cells on glass," *Scientific Reports* 7(1), 2658 (2017).

[14] G. Koppel, D. Eisenhauer, B. Rech and C. Becker, "Combining tailor-made textures for light in-coupling and light trapping in liquid phase crystallized silicon thin-film solar cells," *Opt Express* 25(12), A467-A472 (2017).

[15] A. Zohar, N. Kedem, I. Levine, D. Zohar, A. Vilan, D. Ehre, G. Hodes and D. Cahen, "Impedance Spectroscopic Indication for Solid State Electrochemical Reaction in (CH3NH3)PbI3 Films," *J. Phys. Chem. Lett.* 7(1), 191-197 (2015).

[16] Q. Wang, J.-E. Moser and M. Graetzel, "Electrochemical Impedance Spectroscopic Analysis of Dye-Sensitized Solar Cells," *J. Phys. Chem. B* 109(31), 14945-14953 (2005).

[17] K. Khadga Jung, K. Loni, H. M. Andrew and T. Pullerits, "Phase-synchronous detection of coherent and incoherent nonlinear signals," *Journal of Optics* 18(1), 015504 (2015).

[18] K. J. Karki, M. Abdellah, W. Zhang and T. n. Pullerits, "Different emissive states in the bulk and at the surface of methylammonium lead bromide perovskite revealed by two-photon micro-spectroscopy and lifetime measurements," *APL Photonics* 1(4), 046103 (2016).

[19] V. A. Osipov, X. Shang, T. Hansen, T. n. Pullerits and K. J. Karki, "Nature of relaxation processes revealed by the action signals of intensity-modulated light fields," *Phys. Rev. A* 94(5), 053845 (2016).

[20] S. Fu, A. Sakurai, L. Liu, F. Edman, T. Pullerits, V. Öwall and K. J. Karki, "Generalized lock-in amplifier for precision measurement of high frequency signals," *Rev. Sci. Instrum.* 84(11), 115101 (2013).

[21] K. Karki, M.Torbjörnsson, J. R. Widom, A. H. Marcus and T. Pullerits, "Digital cavities and their potential applications," *J. Instrum.* 8(05), T05005 (2013).

[22] A. Jin, S. Fu, A. Sakurai, L. Liu, F. Edman, T. Pullerits, V. Öwall and K. J. Karki, "Note: High precision measurements using high frequency gigahertz signals," *Rev. Sci. Instrum.* 85(12), 126102 (2014).

[23] F. Fabregat-Santiago, G. Garcia-Belmonte, I. Mora-Sero and J. Bisquert, "Characterization of nanostructured hybrid and organic solar cells by impedance spectroscopy," *Phys. Chem. Chem. Phys.* 13(20), 9083-9118 (2011).

[24] J. Carstensen, E. Foca, S. Keipert, H. Foell, M. Leisner and A. Cojocaru, "New modes of FFT impedance spectroscopy applied to semiconductor pore etching and materials characterization," *Phys. Status Solidi A* 205(11), 2485-2503 (2008).

[25] J. F. Rubinson and Y. P. Kayinamura, "Charge transport in conducting polymers: insights from impedance spectroscopy," *Chem. Soc. Rev.* 38(12), 3339-3347 (2009).